The Relationship between Overlying Synoptic-Scale Flows and Winds within a Valley

C. DAVID WHITEMAN AND J. CHRISTOPHER DORAN

Pacific Northwest Laboratory, Richland, Washington

(Manuscript received 18 January 1993, in final form 16 April 1993)

ABSTRACT

The relationship between winds above and within the Tennessee Valley is investigated climatologically and with an atmospheric numerical model. For the climatological analyses, winds above the valley were determined by interpolation from four surrounding rawinsonde stations, while winds within the valley were measured on four 100-m towers. Tennessee Valley winds are generally weak and bidirectional, oriented along the valley's axis. The valley wind direction depends strongly on the component of the synoptic-scale pressure gradient that is superimposed along the valley's axis at ridge-top level, with winds blowing along the valley's axis from high toward low pressure. This relationship between winds above and within the valley can result in countercurrents similar to those observed in the Rhine Valley. While winds in the Tennessee Valley are driven primarily by this pressure-driven channeling mechanism, downward momentum transport can cause afternoon winds within the valley to approach the wind directions aloft when winds at ridge-top level are strong, and thermally driven valley circulations can appear at night when winds at ridge-top level are weak. A hydrostatic numerical model was used to provide additional insight into the physical processes governing the near-surface winds in the Tennessee Valley. The results support the identification of pressure-driven channeling, downward momentum transport, and thermal forcing as the principal mechanisms determining valley wind directions. They also illustrate the importance of topographical features in producing deviations from simple pressure-driven channeling. The relative importance of thermally driven and pressure-driven winds is examined, and guidelines are presented for estimating when one or the other process will dominate.

1. Introduction

The interaction of winds in a valley with winds above the valley is of interest for both practical and theoretical reasons. For example, the prediction of the dispersion of pollutants released at the ground or from elevated smokestacks in a valley requires the ability to relate local valley circulations to ambient synoptic conditions. While empirically derived relationships may be useful, it is also desirable to develop an understanding of the mechanisms responsible for the observed behavior. In this article we combine results from analyses of measurements and model-generated data to provide insight into factors affecting the climatology of the winds in the Tennessee Valley.

We begin by considering four mechanisms that can produce distinct relationships between winds above and within a valley. The mechanisms can be illustrated in terms of the relationship between the within-valley and above-valley (geostrophic or ambient) winds they will produce, as summarized in Fig. 1.

The first process to be considered is thermal forcing. According to this mechanism, the within-valley winds do not depend on wind directions above the valley but, rather, are generated by locally developed along-valley pressure gradients. These pressure gradients are produced hydrostatically from temperature differences that form along the valley axis, and are a feature of the meteorology of many valleys (e.g., Whiteman 1990). Such locally driven thermal wind systems produce up-valley winds during daytime and down-valley winds during nighttime and are commonly observed in areas with large diurnal cycles in surface sensible heat fluxes, especially under conditions when upper-level winds are weak. Figure 1 illustrates the idealized dependence of valley wind direction on ambient wind direction that would result from this mechanism, assuming a valley axis that runs northeast–southwest, as in the Tennessee Valley.

A second possibility is that strong downward transport of horizontal momentum from above the valley would produce wind directions within the valley that are similar to the geostrophic wind directions aloft (Fig. 1). This downward transport, for example, could be caused by vertical turbulent mixing or by gravity waves. Because of friction, a slight turning ($\sim 25°$) of the geostrophic wind toward lower pressure would be expected as the ground is approached. Downward turbulent transport of momentum would be most likely to occur during unstable or neutrally stratified conditions in wide flat-bottomed valleys with low sidewalls. In such

Corresponding author address: Dr. C. David Whiteman, Battelle Pacific Northwest Laboratory, P.O. Box 999, Richland, WA 99352.

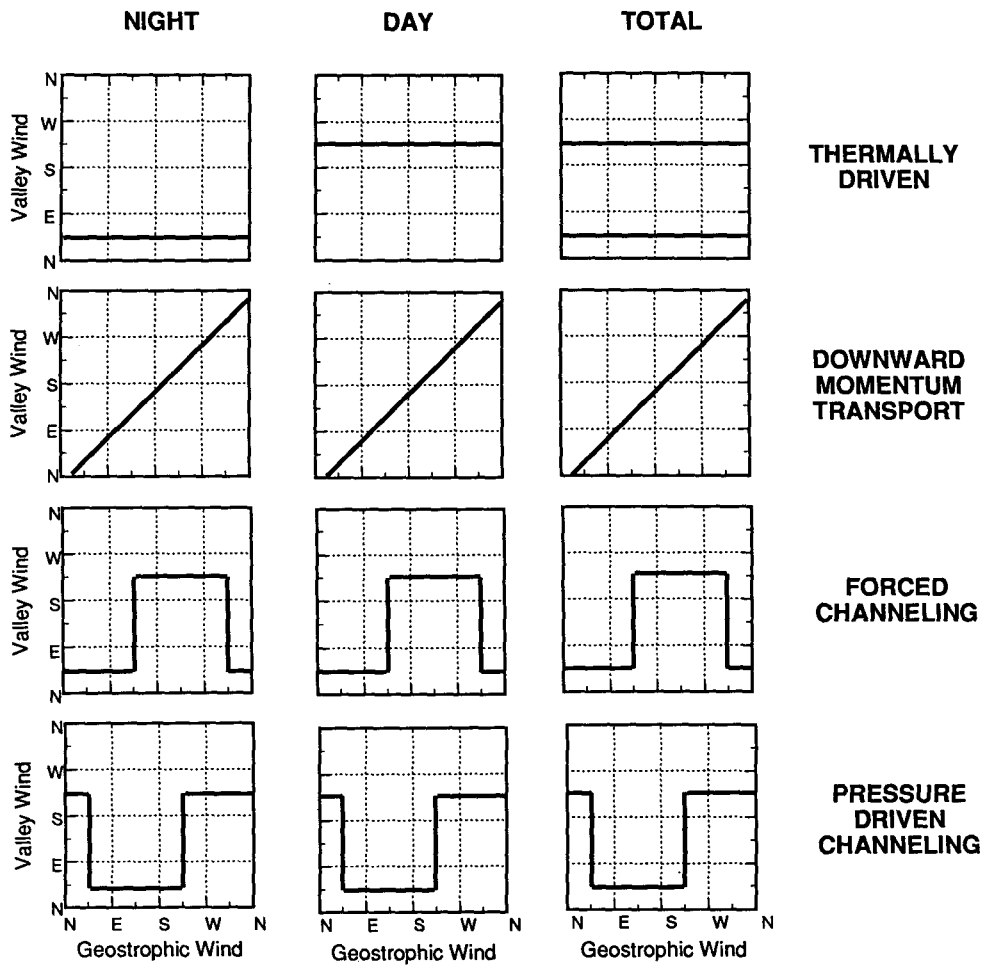

FIG. 1. Relationships between above-valley (geostrophic) and valley wind directions for four possible forcing mechanisms: thermal forcing, downward momentum transport, forced channeling, and pressure-driven channeling. The valley is assumed to run from northeast to southwest.

valleys, thermally driven winds would be less likely to develop, and channeling along the valley axis by the valley sidewalls would be relatively ineffective.

A third possibility is that the ambient winds, which are in geostrophic balance above the valley, will be channeled by the valley sidewalls so that, within the valley, the winds will align with the valley axis. The valley wind direction and speed depend on the sign and magnitude of the component of the ambient wind projected along the valley's axis. In this scenario, winds would blow up or down the valley's axis, depending on the direction of the geostrophic wind relative to that axis. The relationship between valley and ambient wind directions (Fig. 1) produced by the forced channeling results in winds that are predominantly along the valley axis but with sudden shifts in direction when geostrophic winds shift across a line normal to the valley axis.

The fourth process we wish to consider is that of pressure-driven channeling, in which the winds in the valley are driven by the component of the geostrophic pressure gradient along the valley's length. This mechanism was initially proposed by Fiedler (1983) and was used by Gross and Wippermann (1987) to explain narrow bidirectional wind direction frequency distributions observed in Germany's wide Rhine Valley; the resulting behavior is shown in Fig. 1. The along-valley component of the pressure gradient force will be zero only when the geostrophic wind is directed along the valley's axis (i.e., from the northeast or southwest in the figure). Winds in the valley will shift from up to down valley or from down to up valley when the geostrophic wind direction shifts across the valley axis. Thus, pressure-driven channeling will result in winds blowing predominantly along the valley axis, as in the case of forced channeling, but the valley wind reversal will occur for geostrophic wind directions 90° different from those characteristic of the forced channeling mechanism. A remarkable feature of pressure-driven channeling, illustrated in Fig. 1, is that winds in the

valley can blow in opposition to along-valley wind direction components above the valley (e.g., winds in the valley blow from southwest when winds aloft are from northeast). Such valley winds, called *countercurrents,* have been discussed by Wippermann and Gross (1981), Wippermann (1984), and Gross and Wippermann (1987).

In practice, these four mechanisms (or others not considered here) may contribute in varying degrees to the climatology of a given valley. The Tennessee Valley is wider than the Rhine Valley and its depth is substantially greater. Thus, it was not apparent that the pressure-driven channeling found in the Rhine Valley would be found in the Tennessee Valley as well. The moist climatic environment suggested that the diurnal cycle of sensible heat would be substantially smaller than for valleys in the western United States, where thermally driven flows frequently occur. Finally, as noted below, valley winds are often light so that downward momentum transfer might be expected to be relatively unimportant in determining valley wind directions. In the following discussion, we attempt to identify the principal features that determine the wind behavior in the Tennessee Valley.

From Fig. 1, distinct differences in the relationships between valley and ambient wind directions are expected for each of the above four mechanisms. Our approach is to examine the wind direction joint frequency distribution for the Tennessee Valley and to compare it to the patterns predicted for each of the processes discussed above. Before doing so, it is useful to consider two possible limitations of this method. First, the above descriptions of the mechanisms and their consequences are idealized. Not only will atmospheric data be noisy, but the signal itself may be a combination of contributions from the various physical mechanisms. Second, the four mechanisms may not be exhaustive. Alternative processes may be offered subsequently that will produce different wind direction patterns or, worse, patterns that are indistinguishable from those already mentioned.

It is also useful to compare and contrast some aspects of these mechanisms. Only one of them (thermally driven channeling) produces strong night–day valley wind direction shifts. Day–night static stability variations, however, will also affect the day–night frequency of forced channeling and/or downward transport of horizontal momentum because these processes are more important in unstable and neutral conditions. Moreover, forced channeling is more likely to occur in a narrow valley and would require strong downward momentum transport. In a very wide valley, however, downward momentum transport could affect wind directions without forced channeling. Finally, any of the first three mechanisms might obscure the characteristic behavior associated with pressure-driven channeling.

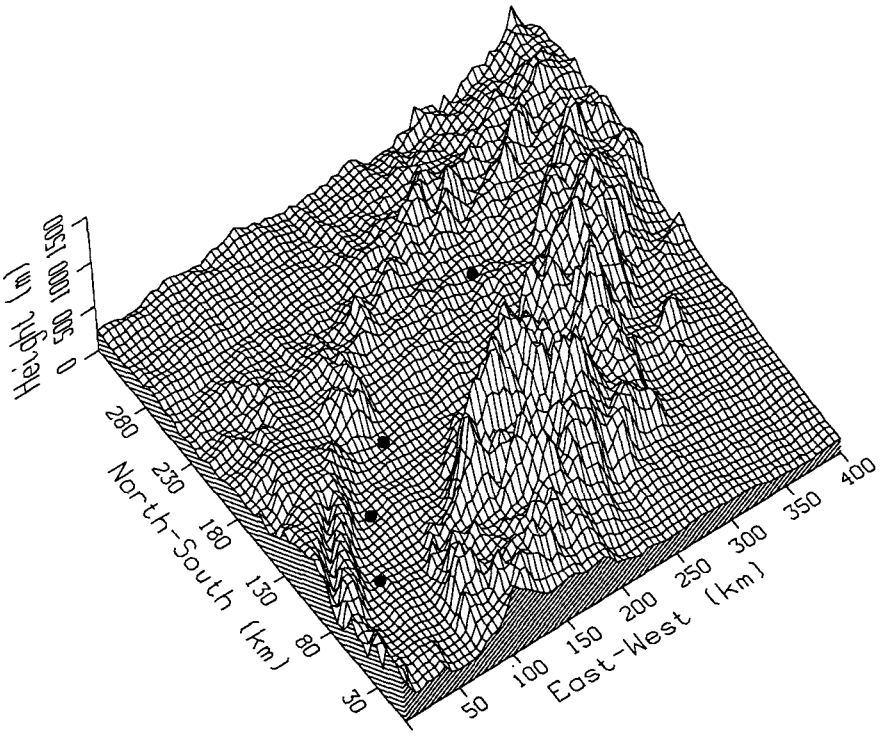

FIG. 2. Topography of the Tennessee Valley, with the locations of the four towers indicated. Towers (top to bottom): Phipps Bend, Oak Ridge, Watts Bar, and Sequoyah.

2. Tennessee Valley topography

The Tennessee Valley is a broad (70 km or more) valley lying between the Cumberland Mountains, rising to the north and west 700 m above the valley floor, and the Great Smoky Mountains to the southeast, whose highest peaks reach as much as 1700 m above the valley floor. In the vicinity of Oak Ridge, Tennessee, the valley is oriented along a 53°–233° axis (i.e., east-northeast–west-southwest). The valley has a relatively flat floor but is "corrugated" by parallel ridges 50–150 m high, spaced 2–3 km apart. The area is heavily wooded with a mixture of deciduous and evergreen trees. West of Oak Ridge the valley curves to the south, while to the northeast of Oak Ridge the valley floor begins to rise more steeply. Figure 2 shows the topography of the area as well as the locations of the tower data sites discussed below.

3. Data

To study the behavior of the near-surface winds, long-term data were obtained from four sites in the Tennessee Valley: the 100-m "X-10C" tower at Oak Ridge National Laboratory (OAK), a 110-m tower at Phipps Bend (PHP), a 93-m tower at Watts Bar (WTB), and a 91-m tower at Sequoyah (SEQ). Rawinsonde data were also obtained for four locations: Athens, Georgia (AHN); Nashville, Tennessee (BNA); Greensboro, North Carolina (GSO); and Huntington, West Virginia (HTS). Data for the four rawinsonde stations and three of the towers were available for the time period January 1984 through December 1988. Tower data for this time period were unavailable at Phipps Bend, and the nearly 4-year period from 17 September 1977 through 31 August 1981 was used instead. Figure 3 shows the locations of the tower and rawinsonde sites. Tables 1 and 2 provide information on the rawinsonde and tower locations, and on the heights of the various wind sensors, respectively.

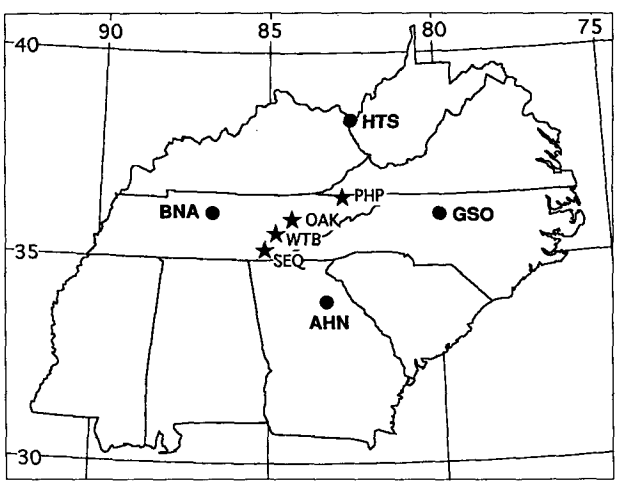

FIG. 3. Locations of rawinsonde stations (circles) and towers (stars).

TABLE 1. Latitudes, longitudes, and elevations of rawinsonde and tower sites.

Station	Latitude (N)	Longitude (W)	Elevation (m MSL)
AHN	33°57′	83°19′	247
BNA	36°07′	86°41′	184
GSO	36°05′	79°57′	270
HTS	38°22′	82°33′	255
PHP	36°29′	82°49′	355
SEQ	35°13′	85°06′	228
WTB	35°36′	84°48′	217
OAK	35°56′	84°19′	262

To estimate the winds above the Tennessee Valley we assumed a geostrophic balance. The geostrophic relationship can be developed from the horizontal equation of motion in pressure coordinates,

$$\frac{d\mathbf{V}}{dt} = -\nabla\Phi - f\mathbf{k}\times\mathbf{V} - \mathbf{F}, \qquad (1)$$

where $\mathbf{V}$ is the vector wind, Φ is the geopotential, $\mathbf{F}$ is a frictional drag term, f is the Coriolis parameter ($=2\Omega \times \sin\phi$), Ω is the angular velocity of the earth (2π day^{-1}), and ϕ is the latitude. In the steady-state case above a valley with negligible surface friction, the winds typically attain an approximate geostrophic balance in which the pressure gradient force is balanced by the Coriolis force such that

$$\mathbf{V} \approx \mathbf{V}_g \equiv \frac{1}{f}(\mathbf{k}\times\nabla\Phi) = \frac{g_0}{f}(\mathbf{k}\times\nabla Z), \qquad (2)$$

where g_0 is the gravitational acceleration and $Z = \Phi/g_0$ is the geopotential height. Geostrophic winds blow parallel to lines of constant geopotential height, with low heights on the left, and the strength of the geostrophic wind is proportional to the horizontal geopotential height gradient.

Geopotential heights at the 85-kPa (850 mb) and 70-kPa (700 mb) pressure levels at the four rawinsonde stations were used in a $1/r^2$ interpolation to estimate the geostrophic winds at the 85- and 70-kPa levels above each of the tower sites using Eq. (2).

The 85-kPa pressure level is typically found at about 1460 m above mean sea level (MSL), an elevation slightly below that of the highest mountains on the

TABLE 2. Tower wind sensor heights.

Tower	Level 1 (m)	Level 2 (m)	Level 3 (m)
PHP	10	60	110
SEQ	9.73	46.56	91.40
WTB	9.72	46.36	93.33
OAK	10	30	100

southeastern side of the valley. The 70-kPa level is at about 3010 m MSL. Geostrophic winds were calculated twice per day using the nominal 0000 and 1200 UTC rawinsonde soundings. Geostrophic winds above the individual towers were subsequently compared to concurrent wind measurements at the towers. The hour-average tower winds at 0600–0700 and 1800–1900 EST were used for the comparison, because these times encompassed the actual rawinsonde release times (2315 and 1115 UTC).

The tower and rawinsonde datasets were of high quality. Rawinsonde and tower data comparisons were possible twice per day for the 5-year period, for a total of 3653 possible comparisons. Only 219 of these occasions (103 morning and 116 afternoon) were missing the 85-kPa geopotential height data at one or more of the four rawinsonde stations. Tower wind data at the nominal 100-m level were missing less than 10% of the time at OAK, SEQ, and PHP, with generally similar availability at the other tower levels as well. Only tower data were available at PHP, and of the 2885 twice-per-day observations, wind data from the 100-m level were missing on only 45 occasions.

The relationships between the rawinsonde ascent times and the local times of sunrise and sunset at Oak Ridge are depicted in Fig. 4. The morning rawinsonde ascents are made before sunrise in some seasons and after sunrise in other seasons. A similar situation occurs with the afternoon soundings relative to sunset. A question therefore arises whether the morning and afternoon ascent times represent nighttime or daytime conditions relative to the development of mountain–valley circulations within the valley, and whether this is a function of time of year. As we shall see, the influence of thermally driven mountain–valley circulations in the Tennessee Valley is rather small. Further, a climatological analysis of the time of reversal of mountain–valley wind flows shows that the reversal times follow sunrise by 4–7 h and sunset by 3–5 h. Such delayed wind reversals are typical of large valleys. For example, the wind reversal in Austria's wide and deep Inn Valley may follow sunrise and sunset by up to 5 h (Dreiseitl et al. 1980; Freytag 1985). Because of the delayed reversal time we conclude that it is a good approximation to associate the 1800 EST data with daytime or unstable conditions and the 0600 EST data with nighttime or stable conditions.

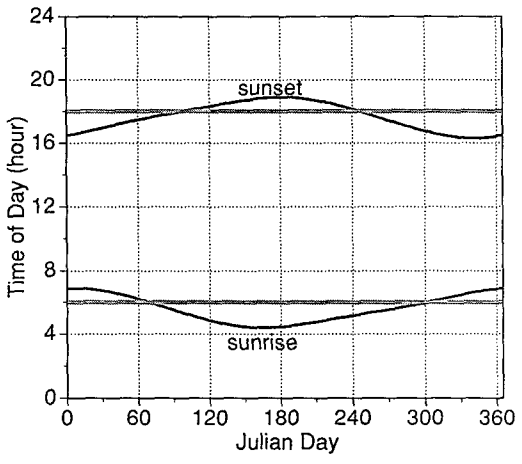

FIG. 4. Sunrise and sunset times at ORNL through the course of a year. The fixed times (0615 and 1815 EST) of rawinsonde launches are shown for comparison.

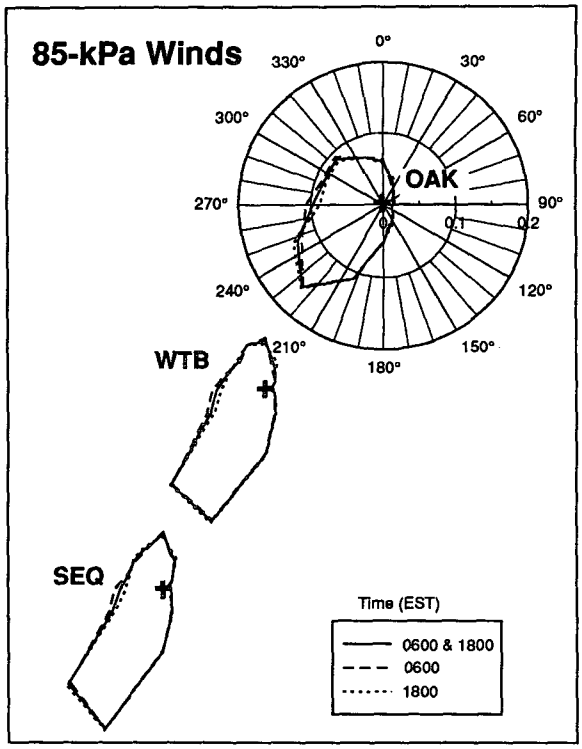

FIG. 5. Wind direction roses for the 85-kPa pressure level for three sites in the Tennessee Valley.

4. Data analysis

In the following discussion, the 85-kPa winds are frequently referred to as ambient or geostrophic winds, and the terms will be used interchangeably. Similarly, winds measured on the tower are referred to as valley winds.

a. Winds aloft

The 85-kPa geostrophic wind direction roses for three of the Tennessee Valley sites are shown in Fig. 5. The winds are predominantly from the two western quadrants with the highest frequency of winds from the southwest—almost directly up the axis of the Tennessee Valley. The median wind speed is 5.9 m s^{-1} and the mean is 6.85 m s^{-1}; the median value corresponds to a geostrophic horizontal pressure gradient of about

0.05 kPa (100 km)$^{-1}$. Wind directions and speeds at the 85-kPa level do not differ significantly between the morning and afternoon soundings. The 70-kPa wind direction frequencies (not shown) are similar to the 85-kPa wind direction frequencies. Both wind speed and direction vary seasonally (also not shown). The median speed at 85-kPa is 8.5 m s^{-1} in winter, 6.9 m s^{-1} in spring, 3.7 m s^{-1} in summer, and 5.4 m s^{-1} in fall. Southwesterly winds have a high frequency in all seasons, while northwesterly winds have a higher frequency in winter than in other seasons. Winds from the east quadrants are more frequent in summer and fall than in winter and spring.

The relationship between wind direction and wind speed at the 85-kPa level is shown for Oak Ridge, Tennessee, in Fig. 6. The strongest wind speeds generally occur when winds are from the south-southwest or southwest; the lightest wind speeds occur when winds are from the east or east-northeast.

b. *Tower winds*

Figure 7 shows the wind roses at the tops of the towers (elevation approximately 100 m) at each of the four sites. There is a strong tendency for winds to lie along the local valley axis, blowing either up or down valley. The broad wind direction distribution for the 85-kPa winds is not seen in the valley winds, and the northeasterly winds found at the surface are almost entirely absent from the 85-kPa wind distributions. The wind directions at the intermediate and lower levels of the towers (not shown) are similar to the wind directions at the tops of the towers, although the wind direction frequency distributions become broader as the base of the tower is approached, probably because of descent into and, often, below the forest canopy.

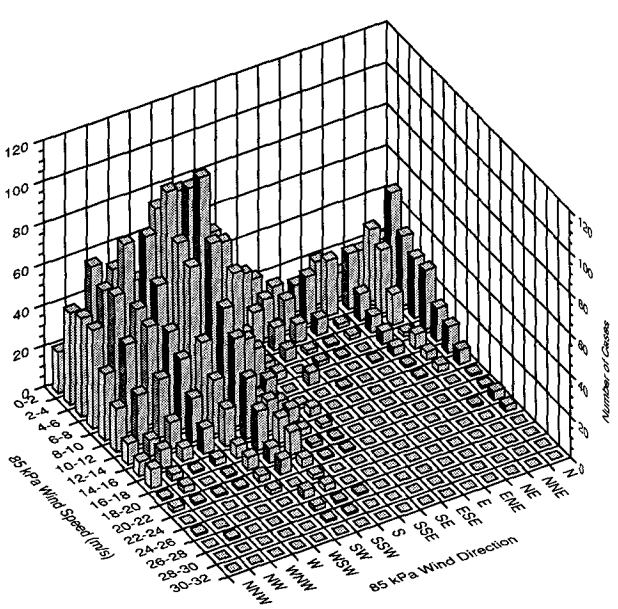

FIG. 6. Joint frequency distribution histogram of 85-kPa wind speeds and directions above Oak Ridge, Tennessee.

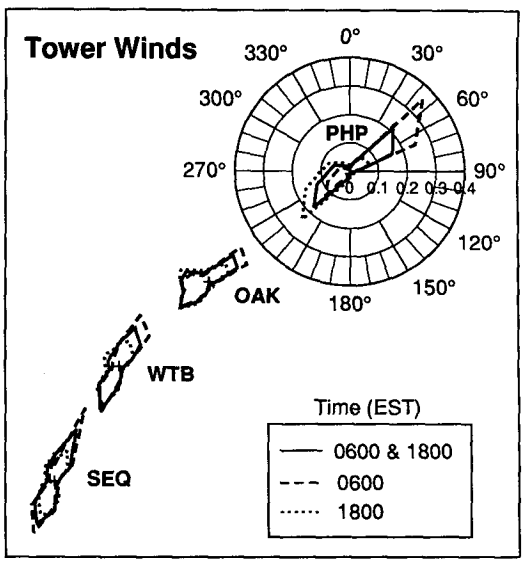

FIG. 7. Wind direction roses at 100 m above ground level for four sites in the Tennessee Valley. At the three sites farthest down the valley, there is little difference between the daytime and nighttime wind roses.

Despite their strong alignment with the valley's axis, the winds in the Tennessee Valley cannot generally be attributed primarily to thermal forcing, because both nighttime and daytime winds have a nearly equal frequency of blowing either up or down the valley's axis. Thus, the valley winds do not satisfy the diurnal characteristic expected from simple thermal forcing as shown in Fig. 1. An exception, however, is the Phipps Bend site, which differs from the other sites in showing a marked tendency for down-valley winds to occur preferentially at 0600 EST and for up-valley winds to occur preferentially at 1800 EST. The Phipps Bend site is located at a higher elevation in the valley where the valley is narrower and the valley floor has a steeper slope, and these features may contribute to the development of thermal winds at the upper end of the Tennessee Valley.

c. *Relationships between ambient and valley winds*

Figure 8 shows the joint probability distribution for 85-kPa and 100-m winds at Oak Ridge, Watts Bar, and Sequoyah. The distribution at Phipps Bend could not be generated because the tower and rawinsonde data periods were not the same at that site. It is instructive to examine the distributions at 0600 and 1800 EST separately because the relative importance of different forcing mechanisms changes with atmospheric stability. Under stable conditions (0600 EST distributions) the valley wind directions clearly separate into two relatively narrow groups, corresponding to up- and down-

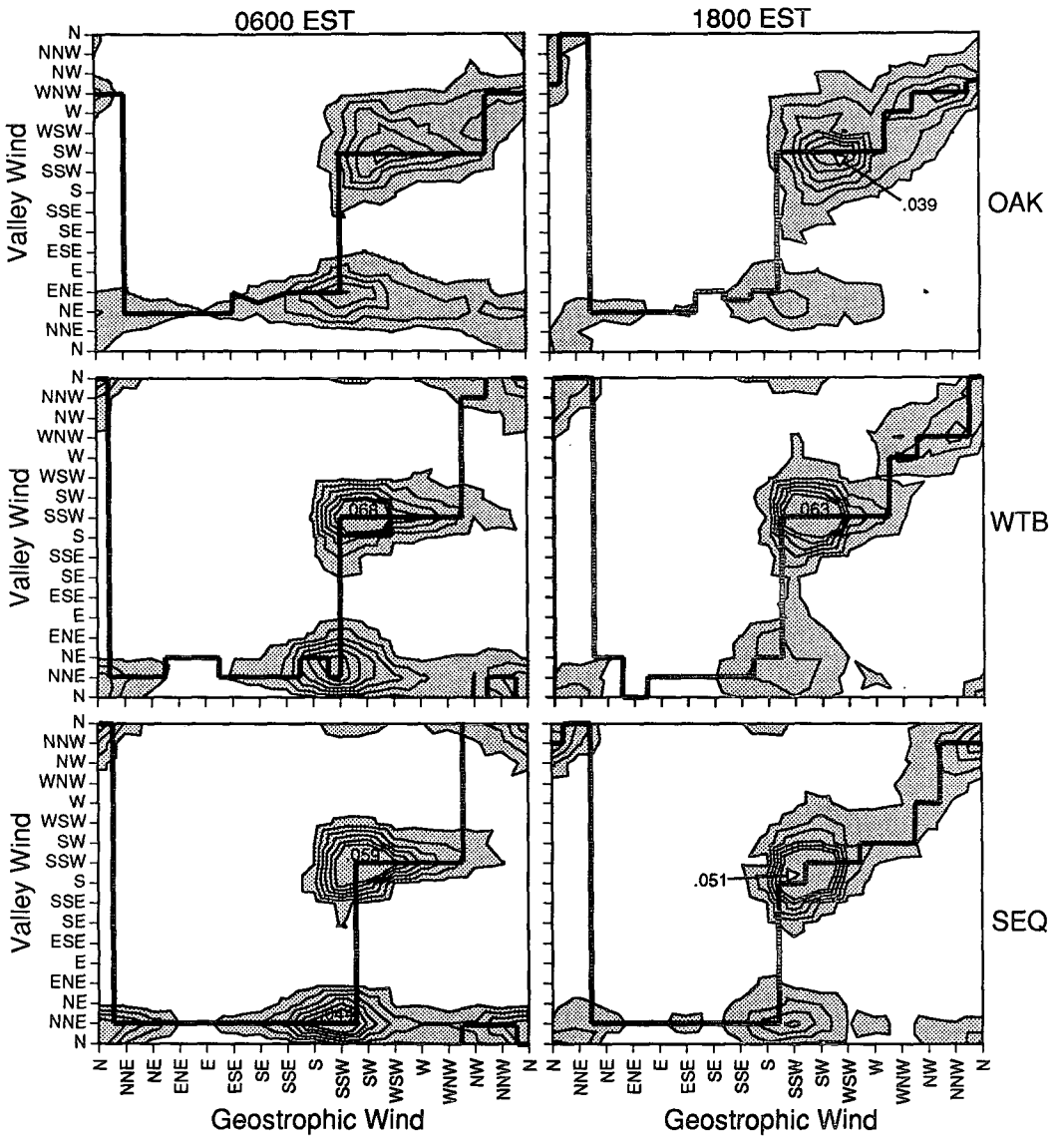

FIG. 8. Joint probability distribution of geostrophic and valley wind directions at Oak Ridge, Watts Bar, and Sequoyah. The solid line shows the locus of maximum probabilities. The shaded area is for probabilities of at least 0.005, contours are at 0.005 intervals to 0.030, and peak probabilities above 0.030 are indicated by labels. Probabilities on the 16 × 16 grid add to 1.00.

valley flows. This feature is particularly evident at Watts Bar and Sequoyah but can also be seen at Oak Ridge. The transition from up-valley (southwest) winds to down-valley (northeast) winds occurs for south to southwest geostrophic wind directions, which is consistent with the behavior expected from pressure-driven channeling. (Ambient winds from the northeast are rarely found in this region, and a corresponding transition between down-valley and up-valley directions is not as well defined.) Exceptions to the pressure-driven channeling behavior are found in the clusters of points in the lower-right-hand corners of the 0600 EST figures. Closer examination of these data shows that they occur predominantly for light ambient winds, which correspond to weak pressure gradients and conditions conducive to the development of nocturnal drainage winds. Thus, pressure-driven channeling seems sufficient to account for the principal feature of the probability distributions at 0600 EST, with some modifications introduced by thermal forcing during periods of light ambient winds.

At 1800 EST, the valley wind directions still divide into two principal groups, but there are some differences from the 0600 EST behavior. The transition between up- and down-valley winds in the centers of the figures is not as sharp as at 0600 EST. Instead, for

south and southwest geostrophic wind directions, the valley wind directions are spread out over a substantially larger range. The principal difference is the greater tendency for the valley wind directions to follow the ambient wind directions when ambient winds lie in the northwest quadrant, and this is particularly true for higher ambient wind speeds. These features suggest that downward turbulent momentum transport is also an important factor in the Tennessee Valley during the daytime. Thermal forcing is not evident in the 1800 EST distributions; although some fraction of the up-valley flows may be enhanced by such a mechanism, the effects would be masked by the response of the valley winds to pressure-driven channeling and the downward momentum transport. These latter two factors appear to be the dominant influences on the 1800 EST valley wind directions.

5. Numerical model

A hydrostatic numerical model was used to provide additional insight into the physical processes governing the near-surface winds in the Tennessee Valley. The model was adapted from one originally developed by Pielke (e.g., Mahrer and Pielke 1977; McNider and Pielke 1984) but modified to incorporate a turbulent exchange scheme based on the prognostic turbulent kinetic energy formulation of Mellor and Yamada (1982). This version of the model has been applied successfully to other complex terrain flow simulations (e.g., Doran and Skyllingstad 1992) and was used in the present case to carry out a series of numerical experiments to examine the response of valley winds to changes in synoptic forcing.

Calculations were done on a $37 \times 32 \times 20$ grid with 11-km horizontal grid spacing and vertical spacing ranging from 10 m at the lowest level to 1000 m at the top of the domain. At the lateral boundaries, the topography was defined to have a zero gradient normal to the boundaries, and the last two grid points at each edge were stretched to move the boundaries far from the interior domain points of interest. The 11-km grid spacing was insufficient to resolve smaller-scale terrain features, such as the corrugations on the valley floor, but it allowed a large number of simulations to be carried out in a reasonable time period while including the main topographic features of the area.

The simulations were designed to identify the primary mechanisms responsible for the observed relationships between geostrophic and valley winds. It is impractical to attempt to simulate all the conditions that contribute to the climatology of the region, but it was possible to choose a set of experiments that illustrate many of the principal features. From the data in Fig. 6, approximately 85% of the 85-kPa winds from north-northeast to southeast have speeds below 6 m s^{-1}, while for winds from south-southwest to north-northwest, 78% of the cases have speeds less than or equal to 8 m s^{-1}. A series of numerical experiments were thus carried out in which the geostrophic winds were fixed at 3, 5, or 8 m s^{-1}, while the directions were varied over a range of angles. An initial stable temperature profile was defined for all tests, and sunrise and sunset times corresponding to early March were chosen. Simulations were begun at sunrise, after an initial 4-h spinup period, and carried out for 24 h. Wind fields at sunset and sunrise the following morning were then selected for analysis.

6. Model results

Figure 9 shows flow patterns at 10 m above ground level (AGL) after 24 h of simulation with a geostrophic wind of 8 m s^{-1} at an angle of 315°. There are significant regions of the valley in which countercurrents—that is, flows opposing the ambient wind—can be found. Figure 10 summarizes the resulting dependence of valley wind direction at 10 m AGL near Oak Ridge on geostrophic wind direction for several wind speeds, where the day and night labels correspond to the 12-h (sunset) and 24-h (sunrise) periods, respectively. Several features are evident in the figure. For daytime winds, there is a tendency for the valley winds to align with the geostrophic winds, as would be expected from downward turbulent momentum transport under well-mixed conditions. At this time, the model shows a nearly adiabatic temperature profile, significant values of TKE, and strong vertical mixing throughout the depth of the valley. However, when the valley atmosphere has cooled overnight, a surface inversion forms, the valley winds near the surface are decoupled from the winds aloft, and the effects of pressure-driven channeling become apparent in the nighttime values (symbols connected with dashed lines). Under these conditions, there is a transition from down-valley to up-valley winds for geostrophic wind directions around 180°. The solid lines in Fig. 10 show the locus of points that would be expected if pressure-driven channeling alone were responsible for the winds' behavior and if the valley were a straight channel oriented along an axis of 53°–233°. When the geostrophic winds are particularly light (2 m s^{-1}), down-valley drainage winds in the vicinity of Oak Ridge are also found, as shown by the point in the lower-right corner of the figure. The simulations also show a much stronger tendency for winds to flow down valley at night in the region near Phipps Bend than for the other tower locations. This is in agreement with the climatological results. The horizontal temperature gradients along the valley are stronger in this area and the katabatic forcing is correspondingly larger.

These features are all in good qualitative agreement with the observations and illustrate the contributions of downward momentum transport, pressure-driven channeling, and thermally forced flows to the climatology of Tennessee Valley winds. There are some discrepancies between simulations and observations. Comparisons of model results with observations ob-

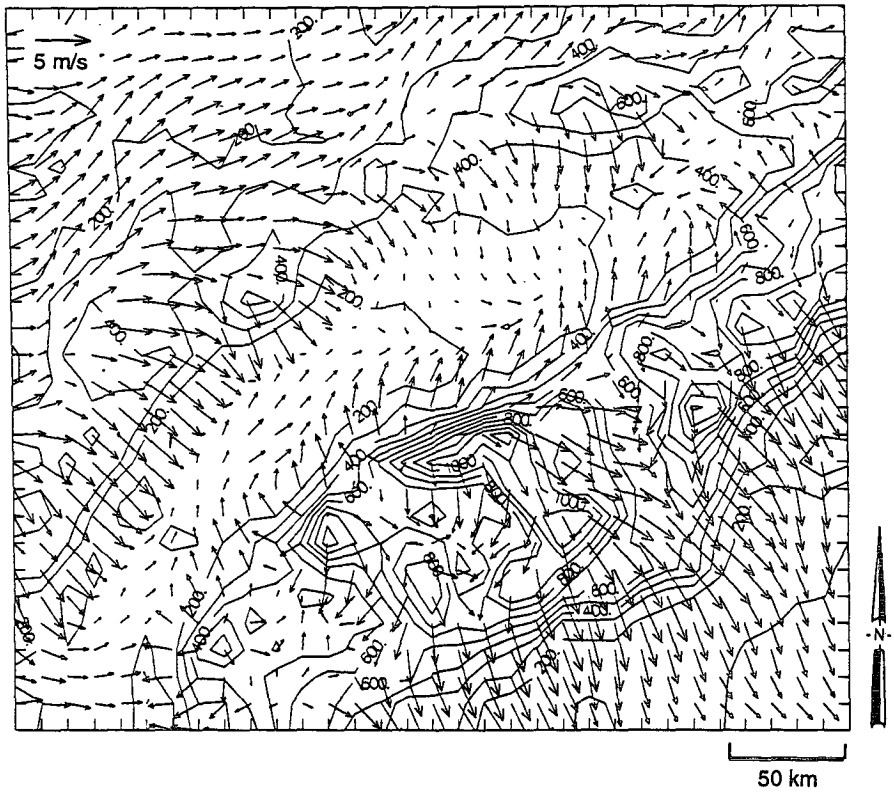

FIG. 9. Simulated wind field at 10 m AGL at dawn (24-h simulation) for 8 m s^{-1} geostrophic wind at 315°.

tained from tethered balloons and rawinsondes flown during a field experiment in the Tennessee Valley in February and March of 1991 (Eckman et al. 1992) show that the simulated valley inversions are shallower than those found in the observations; similarly, in the climatological modeling, the transition between winds aligned with the geostrophic wind directions and winds with directions governed by pressure-driven channeling occurs too close to the surface. This may be partially due to inadequacies of the turbulent parameterization under very stable conditions, but part of the problem may also arise from the model's failure to resolve the numerous low ridges running roughly parallel to the valley's axis. These ridges could produce local channeling of flows and colder pools of air that would not be seen in the simulations.

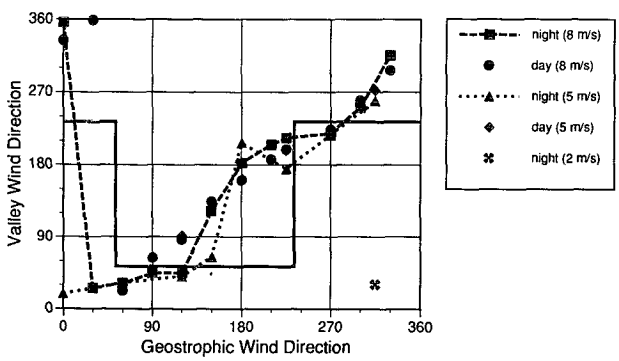

FIG. 10. Simulated valley wind directions as a function of ambient wind directions near Oak Ridge. The solid lines show the locus of points that would be expected if pressure-driven channeling alone were responsible for the wind's behavior and if the valley were a straight channel oriented along an axis of 53°–233°.

In both observations (Fig. 8) and simulations (Fig. 10), the transition from down-valley flows to up-valley flows takes place for ambient wind directions that are to the south of what would be expected for pure pressure-driven channeling. To investigate this effect more fully, several simulations were carried out with idealized terrain configurations that could be used to isolate particular features of the more complicated terrain of the Tennessee Valley and its adjacent mountain ranges. In our first test, two parallel ridges were oriented at a 45° angle, running from southwest to northeast. Each ridge was defined to have a witch-of-Agnesi profile perpendicular to its axis,

$$z = \frac{ha^2}{[(l - l_0)^2 + a^2]}, \qquad (3)$$

where h is 800 m, a is the half-width and equal to 25 km, l is the perpendicular distance from the ridge axis,

and l_0 defines the locus of the ridge axis. The center of the ridge tops was separated by approximately 110 km, and zero-gradient boundary conditions on the topography were imposed, as had been done for the climatological simulations. A geostrophic wind of 5 m s^{-1} from the south was specified, and a 24-h simulation was carried out with the same conditions used for the climatological simulations. After 24 h, the winds on the northwest side of the valley flow down valley (Fig. 11a), as would be expected for pressure-driven channeling. The near-surface winds on the upstream side of the ridge to the southeast exhibit a similar flow pattern, indicating the important contribution of terrain blocking to pressure-driven channeling in the Tennessee Valley. In contrast, Gross and Wippermann concluded that terrain blocking played a minor role in their simulations, which were carried out for much stronger geostrophic winds (13 m s^{-1}) and for a narrower valley (about 35 km in width).

The Tennessee Valley differs from the idealized parallel ridges case in at least two important aspects. The Cumberlands are marked by significant gaps, particularly to the northwest and west of Oak Ridge (cf. Fig. 2), and they are substantially lower than the Smoky Mountains to the southeast. These features were incorporated in two stages by first introducing a gap in the more northern of the two idealized ridges and then reducing the northern ridge height to 600 m while increasing the southern ridge height to 1000 m. For ridges of equal height, the introduction of a gap had little effect on near-surface flows in the valley. However, when the ridge heights were made unequal, the effects were striking (Fig. 11b). The down-valley flows on the northwest side of the valley essentially disappear southwest of the gap. Instead, southerly winds propagate farther north across the valley, and winds tend to flow through the gap. This is consistent with simulations using Tennessee Valley topography, where southerly ambient winds resulted in southerly valley winds near Oak Ridge. It is also consistent with the deviations from idealized pressure-driven channeling behavior that were shown in Fig. 10.

7. Discussion

Our climatological data and modeling simulations for the Tennessee Valley demonstrate the importance of several mechanisms that determine the relationship between valley wind directions and the direction of the winds near ridge-top level. In this section we consider two of these mechanisms, pressure-driven channeling and thermal forcing, in greater detail than has been done up to this point, and discuss their relative importance in other topographic and climatic situations.

According to Gross and Wippermann (1987), pressure-driven channeling is produced as a column of air passes across a valley and expands vertically. The wind velocity decreases, becomes subgeostrophic, and the wind turns to the left in the direction of the imposed large-scale pressure gradient. Within the valley, only the along-valley component of the large-scale pressure gradient can be effective because the air is forced to flow parallel to the valley sidewalls. Although such cases may occur, we suggest an alternate explanation in which the winds in the valley below the ridge line are simply driven by the along-valley pressure gradient component within the valley, as balanced by friction from the valley floor and sidewalls, and constrained by the topography to blow along the valley's axis. This explanation for pressure-driven channeling does not require air to expand into the valley from above, which may be unlikely under conditions of stable stratification, but retains the feature that the winds in the valley are driven by the within-valley horizontal pressure gradient.

The pressure-driven channeling mechanism is illustrated for the Tennessee Valley in Fig. 12. In this figure, the positive x axis is defined in the up-valley direction, and a counterclockwise angle α is defined between the positive x axis and the geostrophic wind vector. With these definitions, which can be applied to a valley of any orientation, the along-valley component of the geostrophic pressure gradient is given by

$$\frac{\partial p}{\partial x} = |\nabla p| \sin\alpha. \tag{4}$$

A geostrophic wind that is perpendicular to the valley ($\alpha = 90$ or 270°, illustrated in Fig. 12a) produces the strongest possible along-valley pressure gradient at ridge-top level and, assuming that no within-valley temperature differences occur to strengthen or weaken the ridge-top pressure gradient within the valley, will produce the strongest flow within the valley, blowing along the valley axis from high toward low pressure. The wind will blow down (up) the valley when $\partial p/\partial x$ is positive (negative). The wind turns to the left as one descends into the valley; alternately, we could say that winds veer or turn clockwise with height above the valley floor. When the geostrophic wind at ridge-top level makes an angle relative to the valley other than 90° or 270° (Fig. 12b), the along-valley pressure gradient is reduced. Unless the pressure gradient at ridge-top level is very strong, the along-valley pressure gradient becomes negligible for angles α near 0° and 180°. Countercurrents occur for $0° \leqslant \alpha \leqslant 90°$ and for $180° \leqslant \alpha \leqslant 270°$ because, in these quadrants, winds in the valley blow in opposition to the along-valley component of the geostrophic wind.

A surprising result from the Tennessee and Rhine valley wind climatologies is the extent to which winds are channeled along the axes of these very wide valleys by the pressure-driven channeling mechanism. In the case of the Rhine Valley, the winds are strongly channeled along the axis of a valley that is 35 km wide with sidewall relief of only about 350 m. In the Tennessee

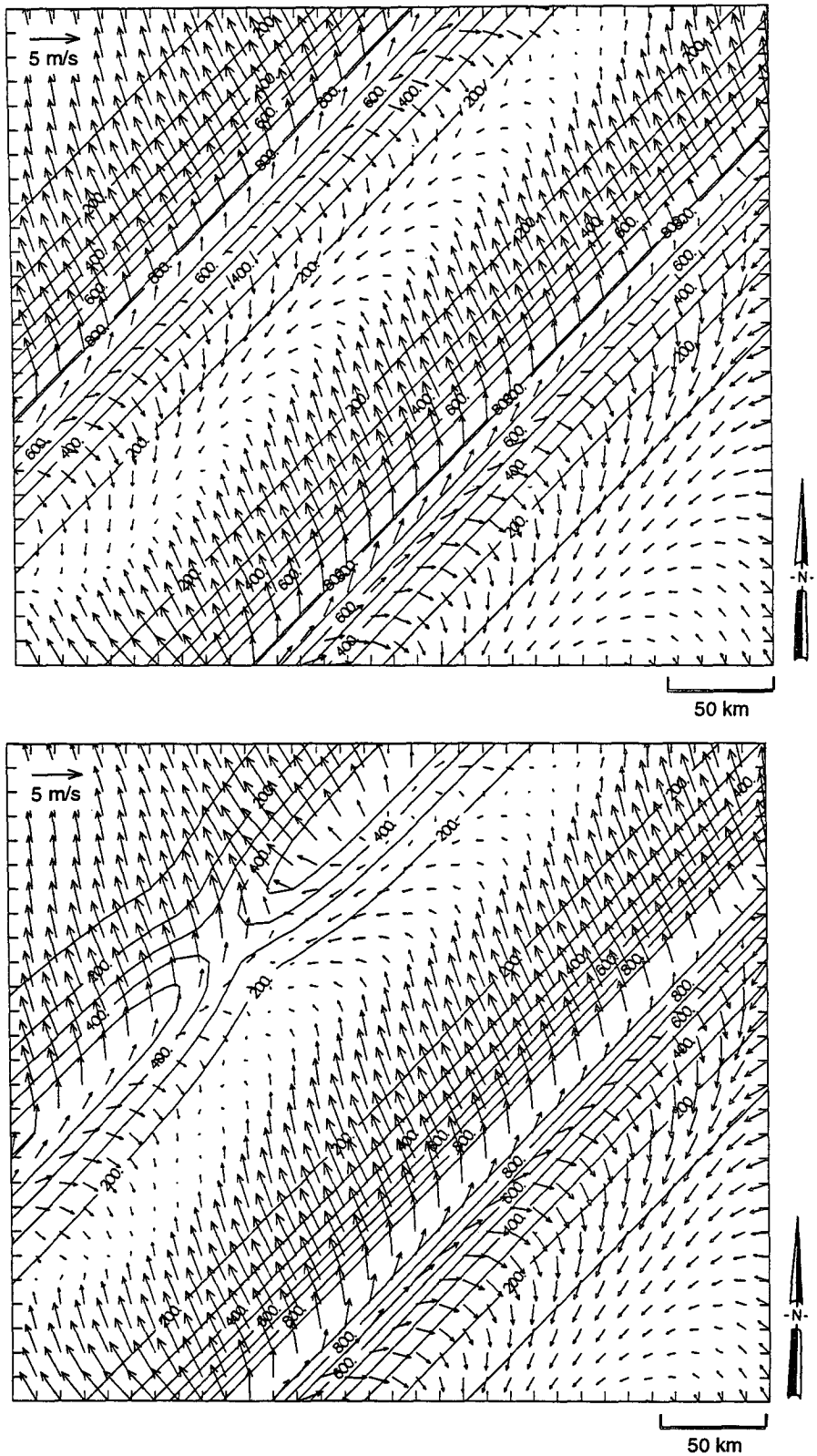

FIG. 11. Simulated wind field at 10 m AGL at dawn (24-h simulation) for 5 m s^{-1} geostrophic wind at 180°. (a) Two parallel ridges, each 800 m high; (b) two parallel ridges, with north ridge 600 m high and south ridge 1000 m high, and a gap in the northern ridge.

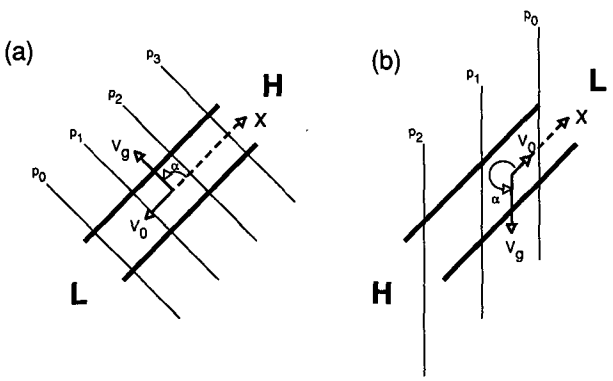

FIG. 12. (a) When geostrophic winds V_g at ridge-top level blow perpendicular to a valley, the along-valley component of the pressure gradient force is maximized, and a within-valley wind V_0 blows along the valley's axis from high to low pressure. (b) Given the same synoptic-scale pressure gradient, the within-valley wind is reduced when the geostrophic wind crosses the valley at an angle. The within-valley wind is still constrained, however, to blow along the valley's axis from high to low pressure. The situation illustrated is an example of a countercurrent, because the within-valley wind blows counter to the along-valley component of the geostrophic wind.

Valley, the sidewalls are substantially higher (700–1700 m), but the valley is also considerably wider (70 km or more). The narrow bidirectional wind frequency distributions (i.e., wind roses) in wide valleys are somewhat counterintuitive. As valleys become wider and shallower, they approximate a plain and might be expected to be less subject to channeling.

The direction and speed of winds in an actual valley depends on the along-valley component of the horizontal pressure gradient at ridge-top level, the modifications to this pressure gradient caused by local cooling and heating processes below the ridge-top level, and the friction imposed by the valley topography. In particular, hydrostatic modifications to the ridge-top along-valley pressure gradient will occur when along-valley temperature differences are present on constant height surfaces within the valley. Such temperature differences can be caused by topographic or energetics variations along a valley's axis. Such variations have been previously investigated by McKee and O'Neal (1989) and have been reviewed and summarized in terms of a topographic amplification factor by Whiteman (1990).

Thermally developed along-valley pressure differences can be expected to be quite weak in shallow valleys because horizontal pressure differences depend strongly on valley depth. For example, consider a valley with a horizontal floor and a constant depth along its length. Assume that the pressure at ridge-top level $p = p_0$ is constant along a valley's length and that there is no along-valley pressure or temperature gradient at this level. An along-valley horizontal pressure gradient will develop within the valley if thermal contrasts develop along the valley's axis. The maximum horizontal pressure difference will occur at the valley's floor, and can be calculated from an integration of the hydrostatic equation, using the expansion $e^x \sim 1 + x$, as

$$\Delta p \approx \frac{gp_0}{R\bar{T}_2\bar{T}_1} D(\bar{T}_2 - \bar{T}_1), \tag{5}$$

where g is the acceleration due to gravity, R is the gas constant, D is the valley depth, and $\bar{T}_1$ and $\bar{T}_2$ are the vertically averaged temperatures (valley floor to ridge top) at two locations along the valley's axis. Assume for simplicity that the valley vertical temperature profiles are linear; we can write the difference in mean temperatures at the sites as

$$\bar{T}_2 - \bar{T}_1 = \frac{(\gamma_1 - \gamma_2)}{2} D, \tag{6}$$

where γ_1 and γ_2 are the vertical temperature gradients at the two sites. Substituting (6) into (5) results in the equation

$$\Delta p \approx \frac{gp_0}{2R\bar{T}_2\bar{T}_1} D^2(\gamma_1 - \gamma_2). \tag{7}$$

The horizontal pressure difference thus depends on the square of the valley depth and linearly on the temperature gradient difference between the two sites. This relationship between pressure difference, valley depth, and temperature gradient difference is plotted in Fig. 13, for $p_0 = 90$ kPa and $\bar{T}_2\bar{T}_1 = 9 \times 10^4$ K^2. From section 4a above, typical synoptic-scale horizontal pressure gradients are on the order of 0.05 kPa (100 km)$^{-1}$. Assuming that the pressure differences shown in Fig. 13 would be expressed over distances of about

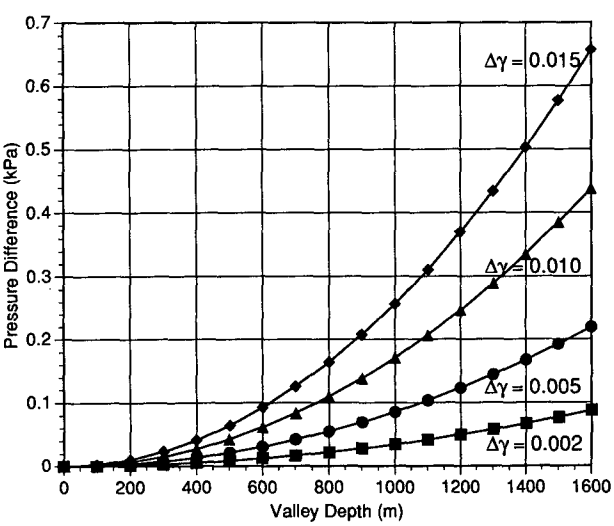

FIG. 13. Pressure difference (kPa) between two locations on a valley floor as a function of valley depth D (m) and vertical temperature gradient difference $\Delta\gamma = \gamma_2 - \gamma_1$ (K m^{-1}). The valley floor is assumed horizontal, and temperature and pressure do not vary along the valley's length at ridge-top level.

100 km and, for illustration, using a temperature gradient difference of 0.005 K m^{-1} (corresponding to a difference in $\bar{T}$ of approximately 1.9 K), we see that a valley would have to be about 750 m deep to produce a hydrostatic pressure gradient equivalent to a typical geostrophic pressure gradient.

Shallow valleys such as the Rhine Valley are unlikely to produce strong thermally driven circulations and are thus especially prone to influence from pressure-driven channeling. The Tennessee Valley is deeper but is located in a moist climatic regime where the within-valley thermal contrasts are small, and the thermally forced winds are also correspondingly weak. In both valleys, pressure-driven channeling then becomes the dominant mechanism that determines valley wind direction, at least for light to moderate ambient winds and stable conditions. In the western United States and in other locations with climates characterized by strong radiational heating and cooling, stronger thermal contrasts can develop within valleys or between valleys and the surrounding plain. Within-valley–above-valley wind relationships in such valleys will be complicated by these within-valley hydrostatically developed pressure gradients, and pressure-driven channeling may be much less evident.

8. Summary and conclusions

We have proposed four mechanisms that can govern the relationship between above-valley and within-valley winds, and have summarized these relationships in terms of plots of above-valley wind directions as a function of within-valley wind directions (Fig. 1). These idealized mechanisms—thermal forcing, downward momentum transport, forced channeling, and pressure-driven channeling—produce very different signatures in such plots. The search for these signatures forms the basis of a climatological and numerical modeling investigation of the processes that determine wind directions in the Tennessee Valley.

Winds within the northeast–southwest-oriented Tennessee Valley are often light, and typically blow either up or down the valley's axis. The winds, except over the sloping terrain at the valley's head, have a nearly equal probability of blowing up or down the valley during both daytime and nighttime, suggesting that thermal wind systems are not a strong feature of the valley's wind climatology. By focusing on the expected patterns in wind direction distributions (above-valley winds versus within-valley winds) produced by different physical processes, we have identified pressure-driven channeling as the dominant mechanism determining near-surface wind directions in the valley for the more common light- and intermediate-strength winds. Downward momentum transport plays an important role when above-valley winds become strong, especially under conditions of weak stability, and thermally driven down-valley flows are evident only when above-valley winds become weak.

Simulations were conducted with a hydrostatic model to investigate further features of the valley wind climatology. These simulations were made by imposing a range of geostrophic wind directions and speeds above the valley and investigating the resulting wind directions within the valley. The simulations supported the conclusion that pressure-driven channeling was the key mechanism influencing Tennessee Valley winds. In addition, the model results provided important detail regarding the spatial variation of winds along and across the valley's axis and illustrated the role of terrain in producing deviations in the behavior of the joint frequency distributions from that expected in a symmetrical, idealized valley. In particular, the difference in heights of the valley sidewalls and the presence of gaps in one of the sidewalls cause southerly winds to propagate farther north across the valley, and winds tend to flow through the gap. These features are seen in the data as well.

With the pressure-driven channeling mechanism, winds in the valley below the ridgeline are driven by the along-valley pressure gradient component within the valley, modified by friction from the valley floor and sidewalls, and constrained by the topography to blow along the valley's axis. Since the geostrophic winds above the valley blow parallel to the isobars and the winds in the valley are constrained to blow along the valley's axis but across isobars, the wind relationships can lead to countercurrents in the Tennessee Valley, in which the within-valley winds blow in opposition to the above-valley geostrophic winds.

Pressure-driven channeling is expected to be a dominant mechanism in valleys under conditions where the influence of the downward momentum transport and thermal wind mechanisms are minimized. This occurs for shallow, but well-channeled, linear valleys in a climatological regime with light to moderate geostrophic above-valley winds and slightly or moderately stable atmospheres. Thermal wind influences would be further minimized by any surface or climatological conditions that reduced the formation of thermal contrasts within the valley. To date, the pressure-driven channeling mechanism has been documented for Germany's Rhine Valley and in the Tennessee Valley. Because of the expected importance of the pressure-driven channeling mechanism for valley air pollution, aerial spraying, and smoke dispersion problems, it should prove useful to extend the research to situations where pressure-driven and thermally driven flows combine to produce valley winds.

Acknowledgments. We thank Drs. R. P. Hosker, Jr. and R. Dobosy for providing the tower data from Oak Ridge National Laboratory, and Mr. N. Nielsen, Mr. H. E. Lindley, and Mr. H. C. Jones of the Tennessee

Valley Authority for providing data from the Watts Bar, Sequoyah, and Phipps Bend power plants. Mr. Glenn Jones assisted with some of the climatological analyses.

Research was supported by the U.S. Department of Energy under Contract DE-AC06-76RLO 1830 at Pacific Northwest Laboratory under the auspices of the Atmospheric Studies in Complex Terrain program. Pacific Northwest Laboratory is operated by Battelle Memorial Institute for the U.S. Department of Energy.

REFERENCES

Doran, J. C., and E. D. Skyllingstad, 1992: Multiple-scale terrain forcing of local wind fields. *Mon. Wea. Rev.*, **120,** 817–825.

Dreiseitl, E., H. Feichter, H. Pichler, R. Steinacker, and I. Vergeiner, 1980: Windregimes an der Gabelung zweier Alpentäler [Wind regimes at the intersection of two alpine valleys]. *Arch. Meteor. Geophys. Bioklim., Ser. B,* **28,** 257–275.

Eckman, R. M., R. J. Dobosy, and W. R. Pendergrass, 1992: Preliminary analysis of wind data from the Oak Ridge site survey. NOAA Tech. Memo ERL ARL-193, Air Resources Laboratory, Silver Spring, Maryland, 45 pp.

Fiedler, F., 1983: Einige Charakteristika der Strömung im Oberrheingraben. *Wiss. Ber. Meteorol. Inst. Univ. Karlsruhe,* **4,** 113–123.

Freytag, C., 1985: MERKUR-Results: Aspects of the temperature field and the energy budget in a large alpine valley during mountain and valley wind. *Contrib. Atmos. Phys.*, **58,** 458–476.

Gross, G., and F. Wippermann, 1987: Channeling and countercurrent in the upper Rhine Valley: Numerical simulations. *J. Climate Appl. Meteor.*, **26,** 1293–1304.

McKee, T. B., and R. D. O'Neal, 1989: The role of valley geometry and energy budget in the formation of nocturnal valley winds. *J. Appl. Meteor.*, **28,** 445–456.

McNider, R. T., and R. A. Pielke, 1984: Numerical simulation of slope and mountain flows. *J. Climate Appl. Meteor.*, **23,** 1441–1453.

Mahrer, Y., and R. A. Pielke, 1977: A numerical study of the air flow over complex terrain. *Contrib. Atmos. Phys.*, **50,** 98–113.

Mellor, G. L., and T. Yamada, 1982: Development of a turbulence closure model for geophysical fluid properties. *Rev. Geophys. Space Phys.*, **20,** 851–875.

Whiteman, C. D., 1990: Observations of thermally developed wind systems in mountainous terrain. *Atmospheric Processes over Complex Terrain, Meteor. Monogr.*, No. 45, Amer. Meteor. Soc., 5–42.

Wippermann, F., 1984: Air flow over and in broad valleys: Channeling and countercurrent. *Contrib. Atmos. Phys.*, **57,** 92–105.

——, and G. Gross, 1981: On the construction of orographically influenced wind roses for given distributions of the large-scale wind. *Contrib. Atmos. Phys.*, **54,** 492–501.